energies

MDPI

Article

Enhanced Density Peak-Based Power Grid Reactive Voltage Partitioning

Xingye Deng [1,*], Canwei Liu [1], Hualiang Liu [2], Lei Chen [3], Yuyan Guo [3] and Heding Zhen [3]

[1] School of Computer Science and Engineering, Hunan University of Science and Technology, Xiangtan 411201, China; canweiliu@mail.hnust.edu.cn
[2] Changde Water Meter Manufacture Co., Ltd., Changde 415000, China; rd01@changdewm.com
[3] School of Information and Electrical Engineering, Hunan University of Science and Technology, Xiangtan 411201, China; chenlei@hnust.edu.cn (L.C.); 2104020326@mail.hnust.edu.cn (Y.G.); 20020401019@mail.hnust.edu.cn (H.Z.)
* Correspondence: dengxingye@hnust.edu.cn

Abstract: Clustering-based reactive voltage partitioning is successful in reducing grid cascading faults, by using clustering methods to categorize different power-consuming entities in the power grid into distinct regions. In reality, each power-consuming entity has different electrical characteristics. Additionally, due to the irregular and uneven distribution of the population, the distribution of electricity consumption is also irregular and uneven. However, the existing method neglects the electrical difference among each entity and the irregular and uneven density distribution of electricity consumption, resulting in poor accuracy and adaptability of these methods. To address these problems, an enhanced density peak model-based power grid reactive voltage partitioning method is proposed in this paper, called EDPVP. First, the power grid is modeled as a weighted reactive network to consider entity electrical differences. Second, the novel local density and density following distance are designed to enhance the density peak model to address the problem that the traditional density peak model cannot adapt to weighted networks. Finally, the enhanced density peak model is further equipped with an optimized cluster centers selection strategy and an updated remaining node assignment strategy, to better identify irregular and uneven density distribution of electricity consumption, and to achieve fast and accurate reactive voltage partition. Experiments on two real power grids demonstrate the effectiveness of the EDPVP.

Keywords: reactive voltage partition; weighted reactive network; density peak

check for updates

Citation: Deng, X.; Liu, C.; Liu, H.; Chen, L.; Guo, Y.; Zhen, H. Enhanced Density Peak-Based Power Grid Reactive Voltage Partitioning. *Energies* **2023**, *16*, 6125. https://doi.org/10.3390/en16176125

Academic Editor: Anna Richelli

Received: 24 July 2023
Revised: 14 August 2023
Accepted: 18 August 2023
Published: 22 August 2023

Copyright: © 2023 by the authors. Licensee MDPI, Basel, Switzerland. This article is an open access article distributed under the terms and conditions of the Creative Commons Attribution (CC BY) license (https://creativecommons.org/licenses/by/4.0/).

1. Introduction

With the rapid advancement of information technology, electricity demand is growing. The electricity consumption load shows the characteristics of regional density. However, the expanding scale and higher voltage levels of the power grid increase the risk of cascading failures in the event of a fault, posing a significant threat to the overall safety and operation of the power grid [1,2]. To address this problem, reactive voltage partitioning [3,4] is proposed. It enables independent voltage regulation for each partition within the power grid, enhancing the controllability of chain failures within each partition and decoupling between different partitions. Therefore, the research on reactive voltage partitioning has important significance.

In recent years, numerous reactive voltage partitioning methods have been proposed. They can be simply classified into two classes. **(1) The first class is the traditional reactive voltage partitioning method.** It primarily relies on geographic location or power grid operation experience for conducting the partitioning. To account for the electrical characteristics of the power grid, researchers utilize reactive voltage to calculate the electrical distance between grid nodes [5–8]. However, these measurement methods often result in

complex computations. To address these issues and enhance partitioning efficiency, researchers have introduced improved particle swarm optimization-based algorithms [9,10] and rapid reactive voltage partitioning methods based on node types [11] for grid node partitioning. While these approaches aim to reduce time complexity, they may lead to lower partitioning modularity. To achieve higher modularity and shorter algorithm computation times, the existing method [12] adopts partitioning based on modularity and utilizes the reactive power support index to assess the rationality of the partitioning. However, it may not effectively ensure sufficient reactive power reserves within the partitioned regions. **(2) The second class is the clustering-based reactive voltage partitioning method.** It represents the mainstream methods used for reactive voltage partitioning. However, certain hierarchical clustering-based methods [13–15] primarily focus on network topology, lacking a comprehensive integration of the electrical characteristics and actual operating conditions of the power grid. Additionally, partitioning clustering-based methods [16,17] may encounter difficulties when dealing with datasets containing non-convex cluster shapes. To address these limitations and achieve a more comprehensive consideration of the density characteristics of the power grid, density clustering-based methods have been proposed. One such method [18] is based on the DBSCAN algorithm. However, it faces performance challenges when dealing with clusters exhibiting uneven density. Another density clustering method [19] is the OPTICS algorithm. It is suitable for dealing with different densities and shapes clustering without hyperparameter constraints, but it is computationally complex and has a high memory footprint.

In summary, the reactive voltage partitioning methods are still immature and require further refinement. Moreover, with the continuous growth in electricity demand, the power grid exhibits two distinctive characteristics:

- **Diverse physical and electrical characteristics of power-consuming entities.** The power grid comprises a diverse array of power-consuming entities with varying types, numbers, and topological arrangements, leading to distinct physical characteristics among these entities. Additionally, the influence of climatic conditions and seasonal variations impacts power consumption, power factor, load fluctuations, and other electrical attributes, resulting in the heterogeneity of electrical characteristics exhibited by these power-consuming entities. Hence, the power-consuming entities in the power grid exhibit a wide diversity of both physical (path hop, node types, etc.) and electrical characteristics (impedance, voltage, etc.).
- **Irregular and uneven density pattern in power load distribution.** The development of society has resulted in different population density distributions across various regions, leading to varying electrical demands in these areas. As a consequence, densely populated regions, such as urban centers, industrial zones, and residential areas usually experience higher power load densities compared to sparsely populated areas, such as suburbs. Moreover, the distribution of populations is characterized by irregularity and unevenness. Consequently, the power load distribution in the power grid also exhibits an irregular and uneven density pattern.

Therefore, the motivation of this paper is to design a more powerful density-based reactive voltage partitioning model, which can consider the different physical and electrical characteristics of power-consuming entities and the irregular and uneven density distribution of power load. To simultaneously consider physical and electrical characteristics, the power grid is remodeled into a new network, by incorporating electrical characteristics into complex networks. To address the challenge of the irregular and uneven density distribution in the power grid, this study optimizes the traditional density peak algorithm, which is well-suited for handling diverse discrete datasets with varying shapes, densities, and distributions. The optimization process involves adapting the clustering model and clustering strategy to be more suitable for the new power grid model. Based on these ideas, an enhanced density peak model-based power grid reactive voltage partitioning method is proposed in this paper, called EDPVP. The main contributions of this paper are as follows:

- A weighted reactive network is constructed to better consider both the physical and electrical characteristics of the power-consuming entities in the power grid.
- An enhanced density peak model with new local density and density following distance is designed to be suitable for weighted reactive networks and the irregular and uneven density distribution of power load.
- A reactive voltage partitioning method is proposed based on the enhanced density peak model, an optimized linear fitting cluster center selection strategy, and an updated remaining node assignment strategy for power grid partitioning quickly and accurately.

The rest of this paper is organized as follows. In Section 2, the prerequisite is presented. Section 3 shows the EDPVP method in detail. Then, the experimental analysis is described in Section 4. Finally, we conclude this paper in Section 5.

2. Prerequisite

2.1. Traditional Density Peak Model

The traditional density peak algorithm [20–22] is a clustering algorithm used for partitioning data into clusters based on their density, which is capable of handling discrete datasets exhibiting a wide range of shapes, densities, and distributions. The core idea of this algorithm is that several density regions exhibit well-defined boundaries in a dataset. And it recognizes that each density region has a high-density point (cluster center) surrounded by low-density points and is relatively far from other cluster centers. To capture the density and distance characteristics, the traditional density peak algorithm introduces two key definitions: local density ρ and density following distance δ. These definitions enable the identification of high-density points and the determination of their relationships with other points. The definitions are as follows.

Definition 1 local density ρ. *The local density ρ of a point represents the number of neighboring points within a specified radius [20]. It can be defined as follows:*

$$\rho_i = \sum_{j \neq i} \chi(d_{ij} - d_c), \tag{1}$$

$$\chi(x) = \begin{cases} 1, & x < 0 \\ 0, & x \geq 0 \end{cases}, \tag{2}$$

where ρ_i is the local density of point i. In general, the larger the local density ρ_i, the more neighbors the point i has, and point i is more likely a cluster center. The d_{ij} is the distance of the points i and j, and d_c represents the cut-off threshold, which is a predefined value used to determine the neighborhood radius for density calculations. The $\chi(x)$ represents the indicator function, which evaluates to 1 when the x is less than 0, and 0 when the x is greater than or equal to 0.

Formula (1) is more suitable for the large-scale dataset. To calculate the local density ρ of a small-scale dataset, the Gaussian Kernels-based local density [20] is defined as follows:

$$\rho_i = \sum_{j \neq i} \exp\left(-\frac{d_{ij}^2}{d_c^2}\right). \tag{3}$$

Definition 2 density following distance δ. *The density following distance δ of a point represents the distance to the nearest higher-density point [21] and can be defined as follows:*

$$\delta_i = \begin{cases} \min\limits_{j}(d_{ij}), & \rho_j > \rho_i \\ \max\limits_{j \neq k}\left(d_{jk}\right), & \rho_i = \rho_{max} \end{cases}, \tag{4}$$

where δ_i is the density following distance of point i. Furthermore, when the ρ_i is the maximum local density, the δ_i is the maximum distance between any two points in the dataset, and the point i is selected as a cluster center.

The selection of the remaining cluster centers should adhere to two criteria: (1) They should exhibit a high local density ρ. (2) The density following distance δ should be relatively large. Hence, the decision value γ of the cluster center [22] can be defined as follows:

$$\gamma_i = \rho_i \times \delta_i. \tag{5}$$

In general, a higher decision value γ_i indicates a greater likelihood that point i is the cluster center. After the selection of cluster centers, the remaining points are assigned to the cluster where their nearest neighbor with a higher density is located.

2.2. The Process of the Traditional Density Peak Algorithm

The process of the traditional density peak algorithm includes the following three steps [23], as shown in Figure 1.

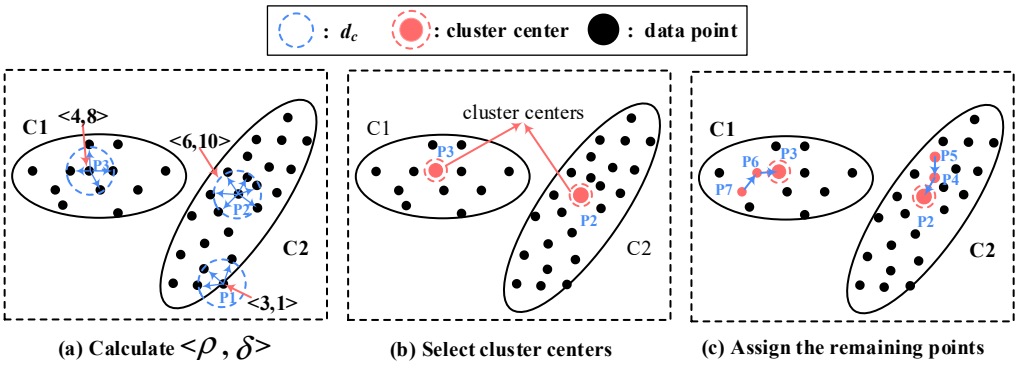


Figure 1. Process of traditional density peak algorithm.

- **Step 1: Calculate local density ρ and density following distance δ.** To begin, the local density ρ is computed for each data point in the dataset using Formula (1) or (3). As illustrated by the blue circles of points P1, P2, and P3 in Figure 1a, Formula (1) is used. Subsequently, the density following distance δ is calculated for each point based on the local densities of all data points. Finally, the local density ρ and density following distance δ of points P1, P2, and P3 have been gained. The red pair in Figure 1a represents the <ρ, δ> pair of the data point.
- **Step 2: Select cluster centers**. Formula (5) is used to calculate the decision value γ of each data point based on the local density ρ and density following distance δ. Then, the data points with the larger decision value γ are selected as the cluster centers. As shown in Figure 1b, the points P2 and P3 are selected as the cluster centers.
- **Step 3: Assign the remaining data points**. Sort all the data points in descending order based on the decision value γ. Then, assign the remaining data points to the cluster of the nearest neighbor with a higher density one by one. As shown in Figure 1c, data points P4 and P5 are clustered to cluster center P2, and data points P6 and P7 are clustered to cluster center P3. Finally, C1 and C2 cluster regions are formed.

3. The EDPVP Algorithm

3.1. Overview

The current partitioning methods that constructed the power grid as the discrete data nodes ignores the relationship between these characteristics of these nodes. To consider the relationship between the characteristics, some methods treat the power grid as an unweighted complex network. However, they overlook the electrical characteristics of the power grid and also disregard the irregular and uneven density distribution of power

load. While the traditional density peak model serves as an efficient clustering method for diverse datasets with varying shapes, densities, and distributions, its applicability is limited to discrete data. To address these problems, this paper tries to develop an enhanced density peak model-based power grid reactive voltage partitioning method, called EDPVP.

(1) To fully consider the physical and electrical characteristics of the power grid and the relationship between these characteristics, we construct the power grid as a weighted reactive network, where the physical characteristics are modeled as a complex network, and the electrical characteristics are modeled as the edge weights of the network. (2) To apply the density peak model to the weighted reactive network, we designed the new local density ρ^{new} and density following distance δ^{new} to enhance the density peak model. (3) To further optimize the performance of reactive voltage partitioning, we have designed an optimized linear fitting cluster center selection strategy and an updated remaining node assignment strategy.

3.2. Weighted Reactive Network Construction

Traditional methods that constructed the power grid as a network solely consider the power grid's topology structural and construct the power grid as an unweighted network. Thus, these approaches do not adequately consider the electrical characteristics of the power grid and fail to achieve effective decoupling of power grid partitioning. To fully consider the physical and electrical characteristics and their relationship, physical characteristics are modeled as a complex network, and electrical characteristics are modeled as edge weights in this paper. In the weighted reactive network, more physical and electrical characteristics are considered, and the relationships between them are integrated.

- **Process of constructing a weighted reactive network.** In power grid partitioning, nodes can be categorized into two main types: reactive power source nodes and load nodes. Reactive power source nodes are PV nodes that provide both active and reactive power in the power grid and typically are generator nodes. While load nodes are PQ nodes, typically users or supply-receiving ends in the power grid. To illustrate this concept, the IEEE-39 bus system is taken as an example, and its node system is simplified into a weighted reactive network, as shown in Figure 2. The busbars are treated as nodes consisting of power sources, substations, and load nodes, also known as PV and PQ nodes. The transmission lines connecting two nodes are treated as the edges in the network, and weights are assigned to them to measure the electrical distance, reflecting the connectivity level between nodes. In this paper, we innovatively use the value of the imaginary part of the node impedance as the edge weights.

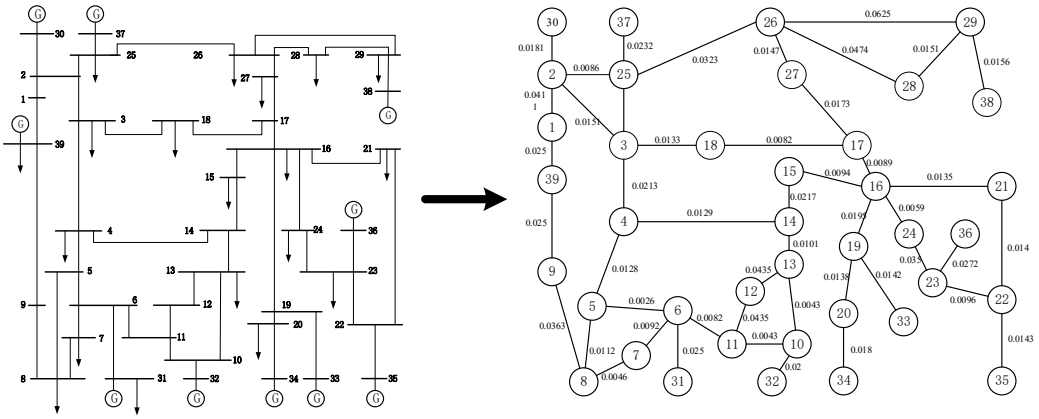


Figure 2. Constructing a weighted reactive power network topology.

- **Edge weights for the weighted reactive network.** Though the network topology mentioned above considers the topology characteristics, the edge weight also should consider both the topology and electrical characteristics of the power grid. This allows

a comprehensive consideration of the electrical coupling relationships between nodes and the degree of correlation between reactive power and voltage in the power grid. Some of the existing methods have employed the sensitivity of reactive power to voltage variations to assess the connectivity between nodes and use it as the weight for the edges. However, these methods involve complex computations, including power flow calculations and iterative processes to determine voltage sensitivity, and may not fully capture the intricate power grid topology. Another method involves using the nodal admittance matrix as edge weights, which reflects the connectivity within the power grid. However, it should be noted that even if two nodes are not directly connected, some electrical linkage between them may still exist between them in practical power grids. Therefore, the method ignores the electrical characteristics of the power grid. To overcome the limitations of the existing methods, this paper proposes a novel approach for reactive voltage partitioning in the power grid. The impedance matrix serves as a suitable representation that captures both the topology and electrical characteristics of the power grid. This paper uses the imaginary part of the nodal impedance matrix to define the edge weights. This is because, in power systems, the physical information contained in the nodal impedance matrix can reflect the electrical coupling relationships between nodes, and the imaginary part indirectly reflects the degree of correlation between reactive power and voltage. Therefore, the weighted reactive network is definite as follows.

Definition 3 weighted reactive network. *For a weighted reactive network topology G = (V, E_w), V is the set of nodes, and E_w is the set of edges. Additionally, W_{ij} is the edge weight between node i and node j, and the edge weight is the value of the imaginary part of the node impedance. The neighbor of node i is V_i, and the common neighbor of node i and node j is V_{ij}.*

The nodal impedance Z_{ij}, between node i and node j, is defined by the following formula:

$$Z_{ij} = \overline{U}_{ij} / I_i, \tag{6}$$

where the incoming current value at node i is denoted as I_i, and the voltage value between node i and node j is denoted as $\overline{U}_{ij}$.

3.3. Enhanced Density Peak Model

The traditional density peak algorithm [24] has more performance for clustering discrete data with irregular and uneven distribution (non-elliptic and non-cyclic) than other cluster methods. But the traditional density peak algorithm is only available for discrete data, and it cannot be directly applied to the weighted reactive network. The main reason is that, on the discrete data, the traditional density peak model utilizes the Euclidean distances between data points to determine local density and density following distance. However, on the weighted reactive network, the distance of nodes cannot be measured by the Euclidean distances. Therefore, it is very necessary to design the new local density and density following distance to enhance the density peak model, to ensure that the enhanced model can be applied to the weighted reactive network.

3.3.1. New Local Density

Local density is the first reason why the traditional density peak model cannot be directly applied to the weighted reactive network. The local density in the traditional density peak model is defined as Definition 1. The local density ρ of a point represents the number of neighbors within a specified radius (Euclidean distance). But the weighted reactive network is a complex network consisting of nodes and edges, where each node has no absolute coordinate and cannot calculate the Euclidean distance. Consequently, the definition of local density ρ does not apply to the weighted reactive network. Therefore, the local density ρ^{new} of the nodes needs to be redefined for the weighted reactive network.

The local density of the traditional density peak model encompasses two essential aspects. Firstly, a high-density point generally possesses greater influence. When a point has high local density, it implies that numerous neighboring points are affected by its presence. Secondly, a high-density point and its neighboring points tend to exhibit strong cohesion, forming a compact and concentrated area within Euclidean space.

Therefore, in the weighted reactive network, the new local density ρ^{new} must satisfy the following two features: (1) A high-density node must have considerable influence, indicating that the node should be followed by multiple low-density nodes. (2) There should be a cohesive relationship between a high-density node and its neighbors, with all of them belonging to the same cluster. To effectively capture these two features, we introduce the notions of node strength and edge strength.

Definition 4 node strength *Vst*. *The node strength can be defined by considering the influence of the node on its neighbors. The more neighbors around a node within a certain region signify a strong influence and higher local density of that node. Nodes with a larger number of neighbors and common neighbors among them imply increased opportunities for power transmission among these nodes. Consequently, nodes positioned at the center of the network tend to exhibit higher node strength. Take node 0 as an example, as shown in Figure 3. Node 0 and its multiple neighbors (1, 2, 3, 4, 5, 6) all share common neighbors, indicating a convergence and gathering of neighbors toward node 0, resulting in stronger interconnections between node 0 and the surrounding nodes. The higher the number of common neighbors that a node shares with its neighbors, the greater the likelihood of these nodes clustering together, thus yielding higher node strength and subsequently greater local density. Therefore, the definition of node strength Vst of node i is as follows.*

$$Vst_i = \sum_{j \in V_i} |V_{ij}| / \sqrt{|V_i||V_j|}, \tag{7}$$

where node j is the neighbor of node i, $|V_{ij}|$ represents the number of elements in V_{ij}, V_{ij} is the common neighbor set of nodes i and j, V_i is the neighbor set of node i, and V_j is the neighbor set of node j.

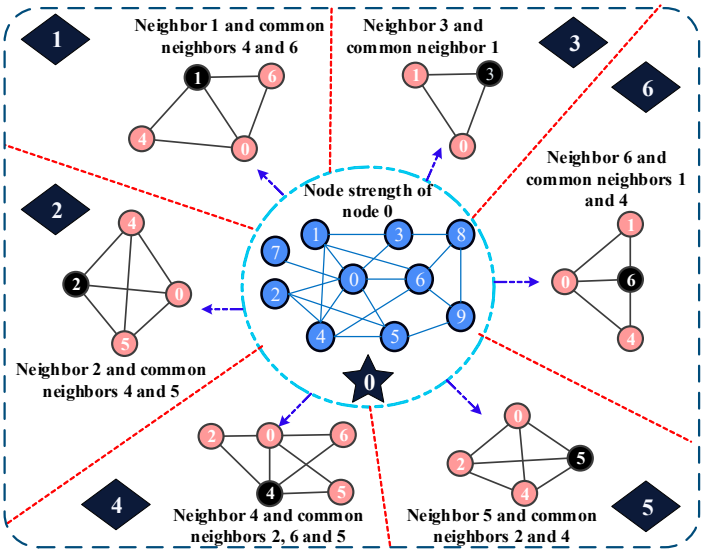


Figure 3. Definition of node strength.

Definition 5 edge strength *Lst*. *Edge strength represents the impact of both direct and indirect edge weight between nodes on the node's local density. Building upon Sun et al.'s concept of neighboring links between nodes [25], it is apparent that relying solely on node strength is insufficient to accurately determine the local density of nodes, as the cohesion among nodes within a region also plays a significant role. Edge weights in the weighted reactive network not only gauge the*

importance of edges but also quantify the strength of connections between nodes, representing the cohesion of nodes. Consequently, we introduce the edge strength to measure this cohesion among nodes. However, it should be noted that the edge strength of the given node is not exclusively influenced by the weights of its directly connected edges. The influence of the edge weights from the common nodes (indirect edge weight) must also be taken into account. Take node 0 as an example, as shown in Figure 4. Its edge strength is determined by the combined impact of the edge weight with each neighbor (1, 2, 3, 4, 5, 6). The edge strength Lst of node i is defined as follows.

$$Lst_i = \sum_{j \in V_i} (A_{ij} + \sum_{z \in V_{ij}} \frac{A_{iz} A_{jz}}{S_z}), \tag{8}$$

where node j is the neighbor of node i, A_{ij} is the edge weight between node i and node j, node z is the common neighbor of node i and node j, and S_z is the sum of all edge weights of node z. Taking node 5 as an example, the process of calculating the effect of node 5 on the edge strength of node 0 is shown in Figure 5.

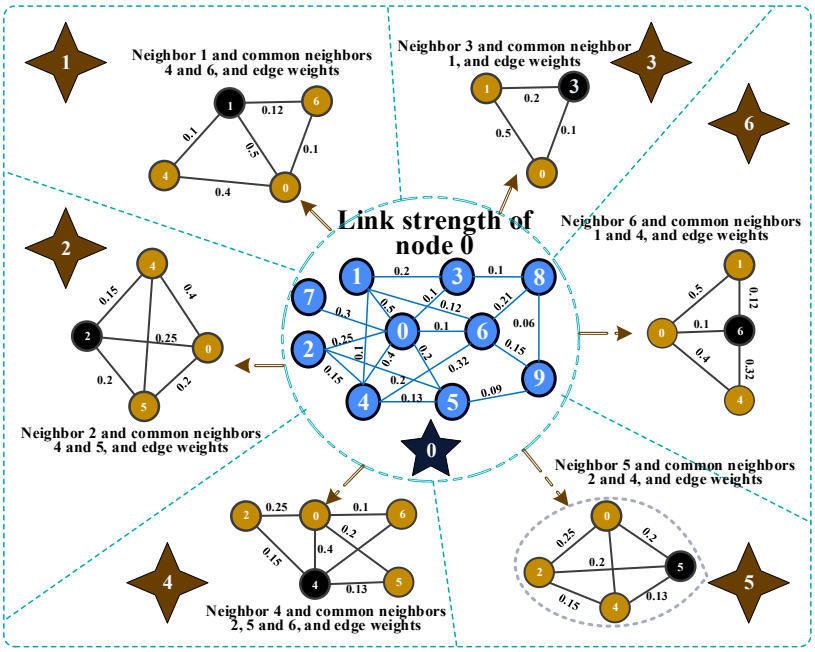


Figure 4. Definition of the edge strength.

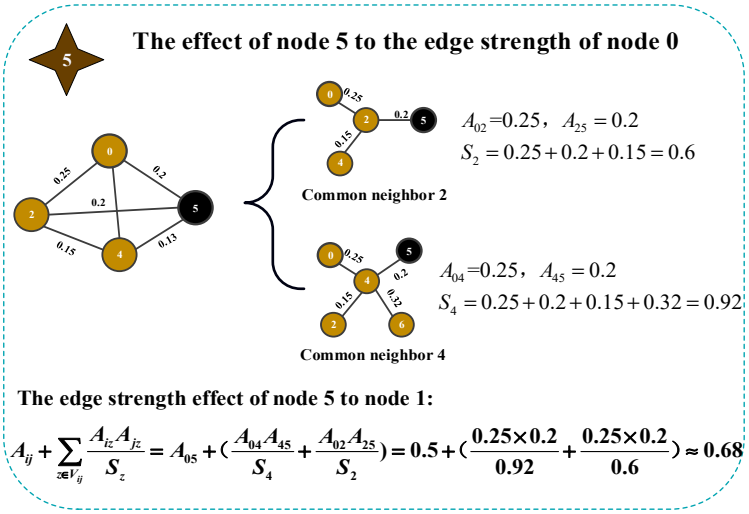


Figure 5. Effect of the neighbor on the edge strength.

Definition 6 New local density ρ^{new}. *In the weighted reactive network, the node's degree serves as an indicator of its level of connectivity and aggregation within the network. Higher node degrees indicate a greater number of connections with other nodes, which in turn suggests the node's higher likelihood of being a cluster center in the network. By combining node degree with node strength and edge strength, we have defined the new local density ρ^{new} applicable to weighted reactive network, as follows.*

$$\begin{array}{l} Vst_i^* = \frac{Vst_i - Vst_{min}}{Vst_{max} - Vst_{min}} \\ Lst_i^* = \frac{Lst_i - Lst_{min}}{Lst_{max} - Lst_{min}} \\ \rho_i^{new} = [\beta \times Vst_i^* + (1-\beta) \times Lst_i^*] \times degree(i) \end{array}, \quad (9)$$

where β is a hyperparameter used to determine the proportion of the node strength and the edge strength in the new local density ρ^{new}. Vst_{max} and Vst_{min} are the maximum and minimum node strengths possessed by all nodes, respectively. Lst_{max} and Lst_{min} are the maximum and minimum edge strengths possessed by all nodes, respectively. Finally, the degree(i) is the degree of node i.

3.3.2. New Density Following Distance

The density following distance is the second reason why the traditional density peak model cannot be directly applied to the weighted reactive network. For discrete data, the density following distance between two nodes is easily obtained by the Euclidean distance, and the distance is unique. However, in the weighted reactive network, nodes are connected by edges. If the density following distance is measured directly based on the measurement in the traditional density peak model. Due to the possibility of multiple paths between two nodes, there can be multiple distances between them, and the edge weights are also ignored. Therefore, the measurement mechanism of the density following distance needs to be redesigned.

Definition 7 new density following distance δ^{new}. *To address these problems, the density following distance of nodes is defined by jointly considering the minimum sum of reactance along all possible paths and the number of hops on the path that has the minimum sum of reactance in the weighted reactive network. Additionally, the reactance is defined as the imaginary part of the node impedance Z, which is the edge weight, as shown in Formula (6). The possible paths P originate from a node and terminate at the neighboring node with a higher density and lower sum of reactance. Taking node 0 as an example, as shown in Figure 6. If among all the nodes in the network, only nodes 5 and 8 exhibit higher local densities than node 0. The red, green, orange, and purple paths are part of the possible paths. It is evidence that the green and purple paths have the minimum sum of reactance in all possible paths. However, there is only one hop on the green path, whereas there are two hops on the purple path. Consequently, node 5 is determined to be the end of the paths, while node 0 is treated as the start of the possible paths, and the hop of the path is 1. Therefore, the density following distance δ_0^{new} of node 0 is 0.2. This distance-measuring method not only captures the electrical characteristics represented by the edge weights but also ensures that the distances between the nodes are unique and easily distinguishable. The definition of the new node distance δ^{new} is as follows.*

$$\begin{array}{c} L_{shortest} = \min\limits_{p \in P} \left(\sum\limits_{l \in p} (\alpha_l) \right) \\ \delta_i^{new} = L_{shortest} \times T_i \end{array}, \quad (10)$$

where $L_{shortest}$ is the minimum sum of the reactance along all possible paths P, p is a path of all possible paths P, l represents an edge of the path p, α_l represents the reactance (weight) of edge l, and T_i is the number of hops of the minimum reactance path starts from node i.

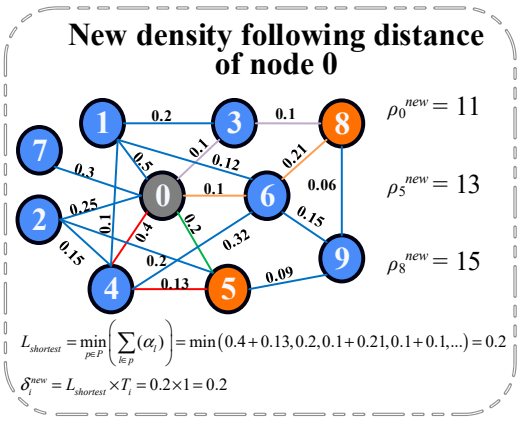


Figure 6. Definition of new density following distance δ^{new}.

3.4. Optimized Reactive Voltage Partition Strategies

3.4.1. Cluster Center Selection Strategy

A critical step in partitioning is the selection of cluster centers. In the traditional density peak algorithm, cluster centers are manually chosen based on the nodes with high local densities and density following distances, as determined through decision diagrams. However, this approach sacrifices the robustness of the density peak algorithm due to it manually selecting the cluster center.

In the traditional density peak algorithm, both the local density and density following distance of the cluster center must be relatively larger. Therefore, to enhance the efficiency and reduce the complexity of reactive voltage partitioning, a filtering process is introduced, eliminating 70% of the nodes with low local densities and density following distances. Subsequently, the new decision value γ^{new} is computed for the remaining nodes. The definition of the new decision value γ^{new} is as follows.

$$\begin{aligned} \rho_i^* &= \frac{\rho_i^{new} - \rho_{\min}}{\rho_{\max} - \rho_{\min}} \\ \delta_i^* &= \frac{\delta_i^{new} - \delta_{\min}}{\delta_{\max} - \delta_{\min}} \\ \gamma^{new} &= \rho^* \times \delta^* \end{aligned} . \tag{11}$$

The decision value γ^{new} of each node is calculated and sorted. Using the IEEE-39 power system standard node as an example, the estimated values γ_{ev} are first calculated using the linear fitting strategy for the node. The estimated value γ_{ev} is defined as follows.

$$\gamma_{ev} = a \times \gamma^{new} + b, \tag{12}$$

where the a and b are hyperparameters.

The results of the linear fitting cluster center selection strategy are shown in Figure 7. By calculating the difference between the estimated and true decision values, and comparing the magnitude of the difference, a more accurate selection of the cluster center for the reactive voltage partition from these filtered nodes can be achieved. The difference value $\Delta\gamma$ is defined as follows.

$$\Delta\gamma = |\gamma^{new} - \gamma_{ev}|. \tag{13}$$

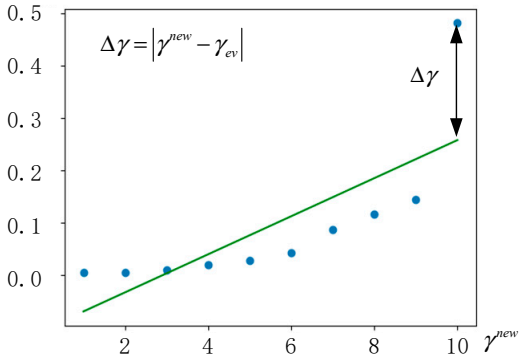


Figure 7. The linear fitting cluster center selection strategy.

When the difference of a node is greater than the average difference, the node is considered more likely to be the cluster center. These nodes, whose differences exceed the average difference, are added to the set of alternative cluster centers. To ensure that there are no two cluster centers in a partition, the nodes with lower local density and density following distance than their neighbors are excluded from the alternative set. Finally, the cluster centers of the weighted reactive network are obtained using this process.

3.4.2. Remaining Node Assignment Strategy

Once the cluster centers have been determined for the weighted reactive network, the remaining nodes are assigned to partitions following a specific procedure, as depicted in Figure 8. To begin, the cluster centers and remaining nodes are sorted based on their local density. Subsequently, lower-density nodes are typically assigned the same partition labels as their higher-density neighbors, signifying their inclusion in the same cluster. The partitioning process unfolds as follows. Firstly, the partition labels are assigned to the neighbors of the cluster centers, leading to the formation of the initial partitions. Next, the unpartitioned nodes acquire partition labels through their partitioned higher-density neighbors. The details are shown in Figure 8. When node 1 is the cluster center and has the highest density, its partition label is assigned to neighbors first, forming the initial partition 1. Then, the partition labels of cluster center node 2 are assigned to the neighbors, forming the initial partition 2. The procedure is continued until all the cluster centers have finished this process. Finally, the partition labels are assigned by the higher-density nodes that have already been partitioned to the unpartitioned neighbors.

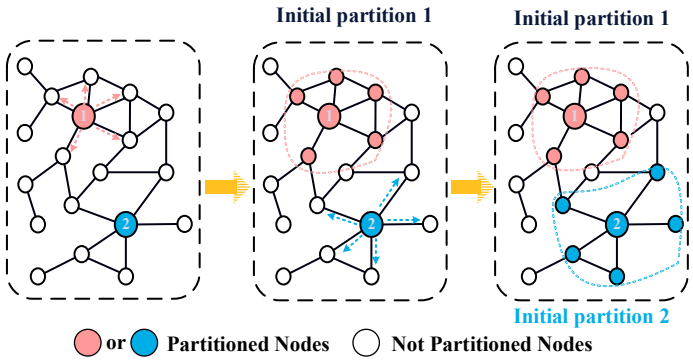


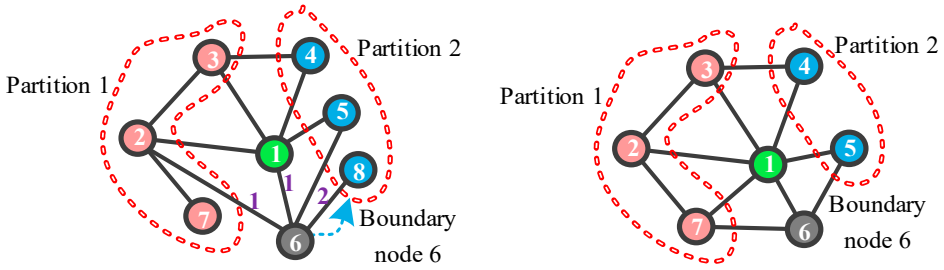
Figure 8. The assignment of remaining nodes.

In the end stage of the above process, when a node is surrounded by several partitions, which is called the partition boundary node, multiple partition labels will be assigned to the partition boundary node. Therefore, determining the correct partition label of the node becomes a problem. In this paper, the partition labels of boundary nodes are determined based on the majority of labels among their neighbors in the weighted reactive network, as shown in Figure 9a. When a boundary node still has multiple partition labels through

the above method, the maximum sum of the edge weights is proposed to resolve this situation, as shown in Figure 9b. It considers both the closeness of the connection between the boundary node and its neighbors and the associated edge weights. The determination of partition label *Pl* of the boundary node is defined by Equation 14, and the partitioning of the boundary node is illustrated in Figure 9.

$$Pl_i = label\left(\max_{r \in R}\left(\sum_{j \in r} W_{ij}\right)\right), \tag{14}$$

where the *label*() represents the partition label, the R is the neighbor partitions set of the boundary node i, r represents the neighboring node set of a partition, and the W_{ij} is the edge weight between node i and node j. The partition label of this boundary node i is the partition label of the neighbor partition that has the maximum sum of edge weights with the node i.



(a) The case of there has only majority partition label.

(b) The case of there has multiple majority partition labels.

Figure 9. Determination of boundary node partition labels.

3.5. Overall EDPVP Steps

In summary, our EDPVP algorithm uses the following steps to perform the reactive voltage partitioning of the power grid.

- **Step 1: Contract the power grid as a weighted reactive network.** The power grid is constructed as a weighted reactive network $G = (V, E_w)$. And, the nodal impedance Z_{ij} is calculated by Formula (6), and the edge weights are the value of the imaginary part of the node impedance Z_{ij}, namely the reactance α.
- **Step 2: Calculate new local density ρ^{new} and density following distance δ^{new}.** The weighted reactive network $G = (V, E_w)$ is inputted into the EDPVP, and the new local density ρ^{new} is computed for each node by Formulas (7)–(9). Subsequently, the new density following distance δ^{new} is calculated for each node by Formula (10).
- **Step 3: Select cluster centers**. The new decision value γ^{new} of each node is computed by Formula (11). Then, the estimated value γ_{ev} and the difference value $\Delta\gamma$ are computed by Formulas (12) and (13), respectively. Finally, based on the linear fitting cluster center selection strategy, the cluster centers are selected.
- **Step 4: Assign the remaining nodes**. Sort all nodes in descending order based on the new decision value γ^{new}. Then, assign the remaining nodes based on the remaining node assignment strategy. Finally, all sub-partitions of the power grid are partitioned.

4. Case Studies

To validate the effectiveness of the proposed EDPVP method, comprehensive case studies have been conducted on two standard power systems: the IEEE 39-bus system and the IEEE 118-bus system.

4.1. Setup

- **Verify metrics.** To ensure the reliability and validity of power grid partitions, it is essential to rigorously verify the partitioning method. In this paper, five metrics as used for verification, which are listed as follows.

(1) Regional connectivity. Regional connectivity [26] refers to the property of a partition where each node has at least one connection to another node within the same partition. In other words, there are no isolated nodes in a partition. During the verification process, if any isolated nodes are identified within a partition, those nodes will be reassigned to the neighboring partition.

(2) Regional reactive power. To ensure static reactive power balance, each partition must satisfy the condition that the sum of the maximum reactive output of the reactive power sources within the partition is greater than or equal to the sum of the reactive loads [27]. The definition of this is as follows.

$$\sum Q_{GC} - \sum Q_L - \Delta Q_\Sigma \geq 0, \tag{15}$$

where the $\sum Q_{GC}$ represents the sum of the reactive power Q_G supplied by generators in the partition and the reactive power Q_C supplied by compensation equipment, the $\sum Q_L$ represents the sum of reactive load, and ΔQ_Σ is the reactive power loss.

Secondly, apart from ensuring regional static reactive power balance, the normal and stable operation of the power system must guarantee sufficient reactive power reserve in each partition. The reactive reserve margin can be calculated using the following formula.

$$\lambda_i = (1 - \frac{Q_{Li}}{Q_{Gi}}) \times 100\%, \tag{16}$$

where λ_i is the reactive power reserve margin in partition i, Q_{Li} is the reactive power required by the load in the partition, and Q_{Gi} is the total reactive power reserve in the region. When $\lambda_i \geq 15\%$, the reactive power reserves in the partition are considered sufficient [28–30].

(3) Regional power grid control. The regional power control index and the regional coupling degree are obtained from the silhouette coefficient S. The silhouette coefficient [31] is often used to reflect the quality of the clustering. Suppose a node system is divided into z partitions denoted as C_i (i = 1, 2, . . ., z). The silhouette coefficient $S(j)$ of node j within the system is defined as follows.

$$S(j) = \begin{cases} \dfrac{\min\limits_{(i=1,2\ldots z)\cap(i\neq j)} \{d_{av}(j,C_i)\} - d_{av}(j,C_j)}{\max\left\{d_{av}(j,C_j), \min\limits_{(i=1,2\ldots z)\cap(i\neq j)} \{d_{av}(j,C_i)\}\right\}}, j \sim C_j, \\ -1, j \nsim C_j \end{cases} \tag{17}$$

where d_{av} (j, C_i) is the average distance from node j of partition C_i to other nodes of partition C_i. The $j \nsim C_j$ represents that node j is not connected with the node in partition C_j. The silhouette coefficient $S(j) \in [-1,1]$, where a higher positive value indicates that the node j matches with the partition C_j, while a negative value indicates that the node j does not match reasonably well with the partition C_j and should be reallocated to another partition.

The power grid control value of node j denoted as $S_G(j)$, is determined by Formula (17), which quantifies the control ability of power node j over the load nodes within its partition. The average value of all power node controls within partition C_j is defined as the regional power control index $\alpha(C_j)$, as follows.

$$\alpha(C_j) = \frac{1}{m_j} \sum_{j \in C_j} S_G(j), \tag{18}$$

where m_j represents the number of the power nodes in the partition C_j.

(4) Regional coupling degree. The regional coupling degree is defined as the average value of the silhouette coefficient S of all the nodes within a partition, and its formula is as follows.

$$\beta(C_j) = \frac{1}{n_j} \sum_{j \in C_j} S(j), \tag{19}$$

where $\beta(C_j)$ represents the regional coupling degree of partition C_j, and n_j is the number of nodes in the partition C_j.

(5) Modularity. To better assess the rationality of the divided partitions, Newman et al. introduced the concept of modularity [32] as an index to evaluate the quality of the network division. Modularity represents the difference between the number of edges among nodes within a network and the number of edges that would be expected under random conditions. It indicates the degree of interconnectivity among nodes within a partition and the sparsity of connections between partitions. The definition of modularity is as follows.

$$Q = \sum_{i=1}^{c} (e_{ij} - a_i^2), \tag{20}$$

where c is some case in which the network is divided into n regions, e is a matrix symmetric of n-th order, e_{ij} element represents the ratio of the number of contiguous edges between the i-th region and the j-th region into which the network is divided to the total number of edges in the network, and a_i represents the sum of all elements in a row or column.

- **Baseline.** The baselines are shown in the Table 1. **(1) PSNPM** [33]. The PSNPM is a hierarchical clustering-based method. It constructed the power grid as discrete entities. It takes into account the randomness, correlation, and balance requirements of the network partitioning when the source-load power varies. In addition, the model proposes a scenario compression technique, which considers the maximal reactive power demand of the partitioning to enable the simulation of typical source-load power scenarios. **(2) MSA** [34]. The MSA is a traditional partitioning method. It constructs the power grid as a network adjacency matrix. It involves two stages. The first stage employs a principal component analysis method to determine the optimal number of partitions and to allocate the nodes into each of the partitions. In the second stage, an $N-1$ robust pilot node selection method is presented, which is applied to an automatic voltage control system. **(3) FACP** [35]. The FACP is based on an improved K-means clustering method. It also constructs the power grid as a network adjacency matrix and utilizes the imaginary part of the nodal admittance matrix as the element in a simplified topological model for voltage control partitioning. By analyzing the normal matrix of the partitioning model, the partitioning clustering samples can be obtained directly, thus effectively reducing the algorithm's time complexity while ensuring a local balance of regional reactive power. **(4) ANCE** [36]. The ANCE is based on the ascending clustering method. It constructs the power grid as discrete entities. Additionally, it introduces a novel recursive grid bi-partitioning strategy and aims to efficiently partition the power system into distinct regions to effectively contain the propagation of disturbances and minimize inter-regional interactions.

Table 1. Baselines.

Abbreviations	Full Name
PSNPM [33]	Pilot-bus selection and network partitioning method considering randomness and correlation of source-load power.
MSA [34]	Multivariate statistical analysis-based power grid partitioning method.
FACP [35]	Voltage control partitioning based on normal matrix spectral bisection method.
ANCE [36]	Network partitioning approach for reactive power/voltage control using analytical nodes coupling expressions.

In summary, these baselines differ from EDPVP in two main aspects. **The first aspect is the object.** In the PSNPM and ANCE, the power nodes and load nodes in the power grid are modeled as discrete entities. However, this ignores the relationships between the characteristics of these entities. To consider the relationship between these characteristics, the FACP and MSA utilize the network adjacency matrix to represent the power grid. However, while considering the relationship between the characteristics, these methods do not adequately consider the electrical characteristics of the power grid. To fully consider the characteristics of the power grid and the relationship between them, our EDPVP constructed the power grid as a weighted reactive network. The physical characteristics of the power grid such as node types and path hops are modeled as a network, and the electrical characteristics of the power grid such as reactance and voltage are modeled as the edge weighted. In this case, more physical and electrical characteristics are considered and the relationships of them are also integrated. **The second aspect is the method.** The PSNPM, FACP, and ANCE are based on clustering-based methods for discrete entities. The MSA determines the optimal number of partitions through the principal component analysis method and constructs the power grid as a network adjacency matrix. In our paper, to adapt the irregular and uneven density distribution of power load, the density peak algorithm is selected. However, the traditional density peak algorithm is only adapted to the discrete data, and it cannot be applicable to the weighted reactive network directly. Therefore, our EDPVP enhances the density peak algorithm to make it can be directly applied for the weighted reactive network and not the discrete entities.

4.2. Case 1: The IEEE 39-Bus System

4.2.1. Regional Connectivity

The IEEE 39-bus system is partitioned using the proposed EDPVP method in this paper, resulting in four partitions, as shown in Table 2 and Figure 10. Partition 1 comprises load nodes 8, 9, and reactive power source node 39. Partition 2 consists of load nodes 4, 5, 6, 7, 10, 11, 12, 13, 14, and reactive power source nodes 31, 32. Partition 3 includes load nodes 16, 19, 20, 21, 22, 23, 24, and reactive power source nodes 33, 34, 35, 36. Partition 4 comprises load nodes 1, 2, 3, 17, 18, 25, 26, 27, 28, 29, and reactive power source nodes 30, 37, 38. Each control partition contains both reactive power source nodes and load nodes, and there are no isolated nodes or single reactive power source nodes or load nodes within the partitions. Additionally, the number of partitions is appropriate, demonstrating that the partitioning scheme satisfies the basic requirements of secondary voltage control. The results of the partitioning are visually represented in Figure 10, where blue dashed lines demarcate each control partition. All partitions are connected, and there are no instances of isolated nodes or the unreasonable division of non-adjacent nodes within the same partition. These outcomes confirm the effectiveness of the proposed reactive power partitioning method in this study.

Table 2. Partitions of the IEEE 39-bus system.

Partitions	Nodes in the Partition
Partition 1	8, 9, 39
Partition 2	4, 5, 6, 7, 10, 11, 12, 13, 14, 15, 31, 32
Partition 3	16, 19, 20, 21, 22, 23, 24, 33, 34, 35, 36
Partition 4	1, 2, 3, 17, 18, 25, 26, 27, 28, 29, 30, 37, 38

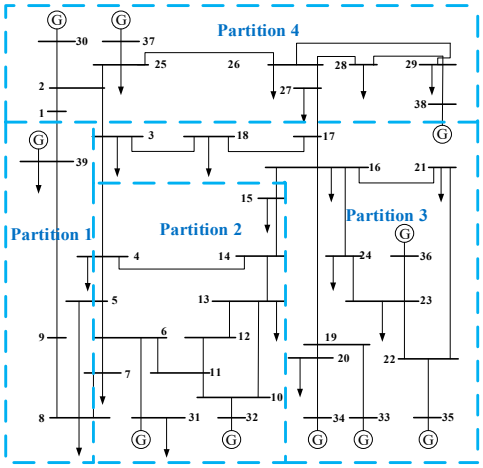


Figure 10. IEEE 39-bus system partition.

4.2.2. Regional Reactive Power

From Figure 11, it can be seen that the sum of the maximum reactive power output of the reactive power supply within partition 1 is 300 Mvar, the sum of the reactive loads of the load nodes within the partition is 176.6 Mvar, and the reactive power reserve margin is 41.13%; the sum of the maximum reactive power output of the reactive power supply within partition 2 is 600 Mvar, the sum of the reactive loads of the load nodes within the partition is 509 Mvar, and the reactive power reserve margin is 15.17%; the sum of the maximum reactive power output of the reactive power supply in partition 3 is 957 Mvar, the sum of the reactive loads of the load nodes in the partition is 334.9 Mvar, and the reactive power reserve margin is 65%; the sum of the maximum reactive power output of the reactive power supply in partition 4 is 950 Mvar, the sum of the reactive loads of the load nodes in the partition is 270.8 Mvar, and the reactive power reserve margin is 71.49%. The reactive power output of each sub-partition of the EDPVP method is greater than the sum of load power in the sub-partition, which satisfies the static reactive power balance of the sub-partition. At the same time, the reactive power reserve in each sub-partition can be guaranteed to be sufficient, meeting the requirement of a 15% reactive power reserve.

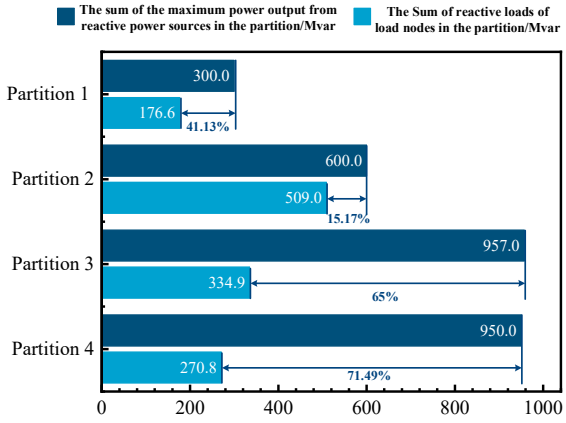


Figure 11. Static reactive power balance test.

4.2.3. Effectiveness Analysis

To demonstrate the superiority of the reactive power reserve of the EDPVP method, a comparison is conducted with two other partitioning methods, PSNPM [33] and MSA [34]. The reactive power reserve results of these methods are evaluated and compared. From the results presented in Table 3, it is evident that the reactive power reserve of Partition 1 in PSNPM is 14.37%, and for Partition 2 in MSA, the reactive power reserve is 8.99%. These

values fall short of the required reactive power reserve of more than 15%. In contrast, the partition reactive power margins obtained using the EDPVP method meet the requirement, ensuring a reactive power reserve greater than 15%.

Table 3. The reactive power reserve of partition methods.

Method	Reactive Power Reserve of Partitioning Methods/%			
	Partition 1	**Partition 2**	**Partition3**	**Partition 4**
EDPVP	41.13	15.17	65.00	71.49
PSNPM [33]	14.37	73.92	23.14	69.23
MSA [34]	41.58	8.99	50.84	27.91

To further illustrate the superiority of the EDPVP method, it is compared with the PSNPM [33] and MSA [34]. The regional power grid control, regional coupling degree, and modularity are used as the evaluation metrics of partitioning quality, and the results are shown in Figure 12 and Table 4.

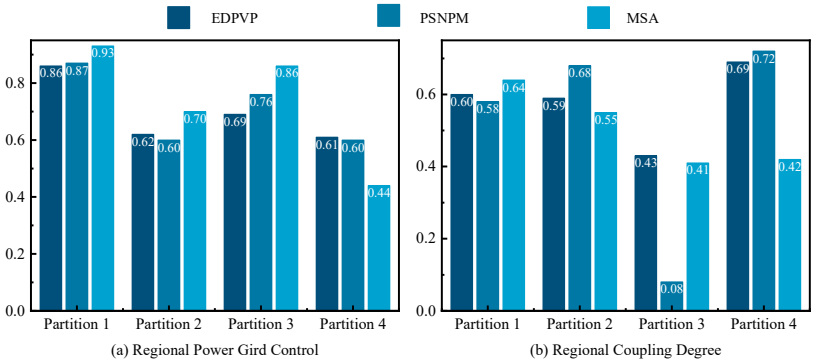


Figure 12. Comparison of partitioning quality.

Table 4. Modularity comparison of partitioning methods.

Partitioning Method	EDPVP	PSNPM [33]	MSA [34]
Modularity	0.58	0.56	0.55

From Figure 12 and Table 4, a comparison of the EDPVP method with the PSNPM and MSA methods reveals the following findings: **(1) Regional power grid control comparison.** In Partition 1 and Partition 3, EDPVP shows slightly lower regional power grid control than the PSNPM by 0.01 and 0.07, respectively. However, in Partition 2 and Partition 4, EDPVP exhibits higher regional power grid control than PSNPM by 0.02 and 0.01. When compared to the MSA, EDPVP demonstrates higher regional power grid control in Partition 4, with a difference of 0.16. Overall, the power control power in each partition is more stable with EDPVP, and there is a strong coupling between the power nodes in the partitions and the partitions where they are located. This indicates that the reactive power nodes can effectively regulate the reactive power of the partition, leading to better control of the node voltage within each partition. **(2) Regional coupling degree comparison.** In PSNPM, the regional coupling degree of Partition 2 and Partition 4 is higher than that of EDPVP by 0.09 and 0.03, respectively, while Partition 3 has a lower regional coupling degree by 0.35 compared to EDPVP. For the MSA, only Partition 1 has a slightly higher regional coupling degree by 0.04 compared to EDPVP, while Partition 2, Partition 3, and Partition 4 have lower regional coupling degrees than EDPVP by 0.04, 0.02, and 0.27, respectively. These results suggest that there are issues in the PSNPM and MSA methods, with the nodes having a lower match with the partition they are located in, and a weak coupling of the nodes within the partition. **(3) Modularity comparison.** The modularity of EDPVP is higher than

that of the PSNPM and MSA, indicating that the tightness between the nodes within the partitions of EDPVP is stronger. In summary, the effectiveness and rationality of the EDPVP method are validated by using regional power grid control, regional coupling degree, and modularity as partition quality evaluation metrics. It also shows that the enhanced density clustering-based method in EDPVP is better than the clustering method in PSNPM, while the weighted reactive network in EDPVP is effective in improving the quality of partitions compared to the unweighted reactive network in MSA.

4.3. Case 2: The IEEE 118-Bus System

4.3.1. Regional Connectivity

The IEEE 118-bus system contains 54 reactive power source nodes and 64 load nodes, which is the power grid of the Midwestern U.S. Then, the method in this paper is used to partition it. The corresponding partitioning results are shown in Figure 13 and Table 5.

Table 5. Partitions of the IEEE 118-bus system.

Partitions	Nodes in the Partition
Partition 1	1–20, 30, 31, 33–39, 43, 113, 117
Partition 2	21–29, 32, 72, 114, 115
Partition 3	82–90
Partition 4	40, 41, 42, 44–71, 73–79, 81, 116, 118
Partition 5	80, 91–112

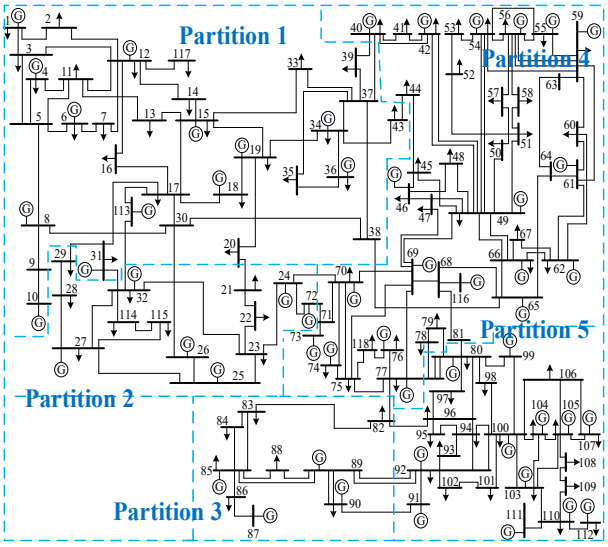


Figure 13. IEEE 118-bus system partition.

The IEEE 118-bus system is divided into five partitions by the EDPVP partition method, each partition with good regional connectivity, and the partitioning results are basically in line with reality. Generator nodes (PV nodes or balancing nodes) are located in each partition to ensure a reliable power supply within each relatively independent power partition.

4.3.2. Regional Reactive Power

As shown in Figure 14, the reactive power output in each partition is found to be greater than the load power in the respective partition, satisfying the static reactive power balance within each partition. Additionally, the reactive power reserve margin of Partition 1 is 78.55%, the reactive power reserve margin of Partition 2 is 96.12%, the reactive power reserve margin of Partition 3 is 92.54%, the reactive power reserve margin of Partition 4 is 83.89%, and the reactive power reserve margin of Partition 5 is 89.84%. All partitions

exhibit reactive power reserve margins greater than 15%, which attains the requirement for reactive power reserves.

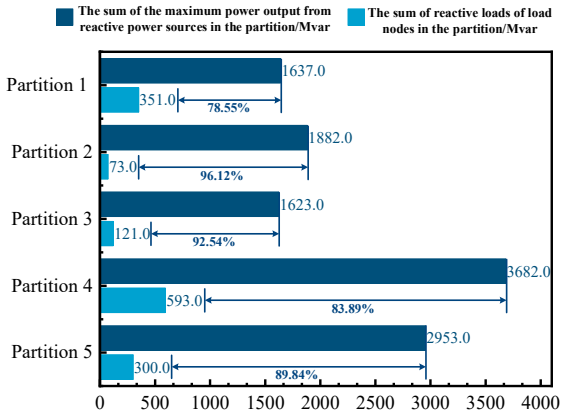


Figure 14. Static reactive power balance test.

4.3.3. Effectiveness Analysis

To demonstrate the superiority of the EDPVP method in the reactive voltage reserve, a comparison is made with the FACP [35] and ANCE [36], as shown in Table 6. The reactive power reserve results in Table 6 reveal that the FACP method fails to meet the reactive power reserve requirement of 15% in Partition 1 (11.26%), Partition 4 (6.15%), and Partition 5 (11.88%). In contrast, the ANCE and EDPVP methods all achieve reactive power reserve margins of more than 15% in all partitions. This comparison clearly illustrates that the EDPVP method outperforms the FACP method in terms of achieving the required reactive power reserve, further validating the effectiveness and superiority of the proposed EDPVP method for reactive power partitioning in power grids.

Table 6. The reactive power reserve of partition methods.

Method	Reactive Power Reserve of Partitioning Methods/%						
	Partition 1	**Partition 2**	**Partition3**	**Partition 4**	**Partition5**	**Partition 6**	**Partition 7**
EDPVP	78.55	96.12	92.54	83.89	89.84	--	--
FACP [35]	11.26	24.78	15.23	6.15	8.17	11.88	22.07
ANCE [36]	54.23	18.75	68.54	--	--	--	--

To further illustrate the superiority of the EDPVP method, it is compared with the FACP [35] and ANCE [36]. The regional power grid control, regional coupling degree, and modularity are used as the evaluation metrics of partitioning quality, and the results are shown in Figure 15 and Table 7.

Table 7. Modularity comparison of partitioning methods.

Partitioning Method	EDPVP	FACP [35]	ANCE [36]
Modularity	0.64	0.61	0.60

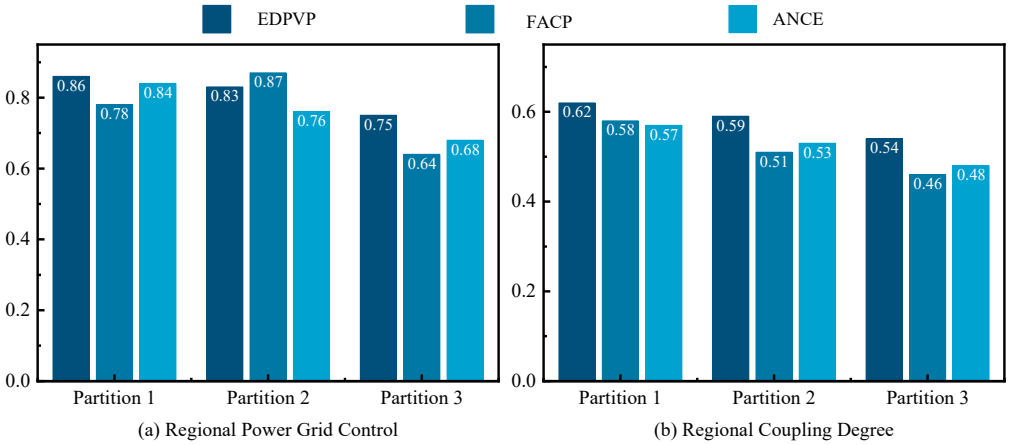


Figure 15. Comparison of partitioning quality.

From Figure 15 and Table 7, a comparison of the EDPVP method with the FACP and ANCE methods reveals the following findings: **(1) Regional power grid control comparison.** The Partition 1 and 3 of the EDPVP is 0.08 and 0.11 higher than in the FACP, while each partition of the EDPVP is 0.02, 0.07, and 0.07 higher than that in the ANCE. This shows that the enhanced density clustering-based method in this paper is more effective than the method in the FACP and ANCE in the grid partitioning. **(2) Regional coupling degree comparison.** Each partition of the EDPVP is 0.04, 0.08, and 0.08 higher than FACP, while is 0.05, 0.06, and 0.06 higher than ANCE. This also shows that the weighted reactive network in this paper is more effective than the unweighted reactive network in the FACP in the grid partitioning. **(3) Modularity comparison.** Compared with the FACP and ANCE, the modularity of the EDPVP is higher 0.03 and 0.04. In summary, these results demonstrate that the power nodes corresponding to the EDPVP effectively control voltage within each partition. Furthermore, the tightly coupled electrical connections within each partition prove the effectiveness of the proposed algorithm.

4.4. Ablation Analysis

In this section, specific components of our proposed method will gradually ablate, and enable us to understand how each component impacts the effectiveness of the partitioning results. The components include the weighted reactive network and the proposed local density ρ^{new} and density following distance δ^{new} of the enhanced density peak model.

4.4.1. Weighted Reactive Network

The construction of the weighted reactive network is an important innovation in this paper. To demonstrate the effectiveness of the construction of the weighted reactive network, we compare the EDPVP with weighted reactive power networks (weighted) and EDPVP with unweighted reactive power networks (unweighted) on the IEEE 39-bus system, where the edge weights of the unweighted reactive power network are all set to 1. The evaluation of partition quality is based on regional power grid control, regional coupling degree, and modularity. The comparison results are shown in Figure 16 and Table 8.

Table 8. Modularity comparison.

Partitioning Method	Weighted	Unweighted
Modularity	0.58	0.49

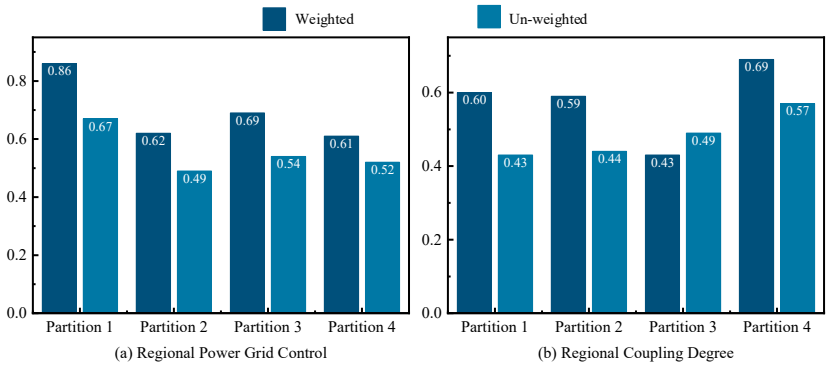


Figure 16. Comparison of the EDPVP with the weighted and unweighted reactive network.

From Figure 16 and Table 8, a comparison of the weighted and the unweighted reveals the following findings: **(1) Regional power grid control comparison.** The weighted outperforms the unweighted in terms of regional power grid control in all partitions, especially for Partition 1, where the metrics are higher 0.19 than the unweighted. **(2) Regional coupling degree comparison.** Weighted demonstrates higher regional coupling degrees in most Partitions compared to the unweighted, except for Partition 3, where the regional coupling degree of the weighted is lower than that of the unweighted by 0.06. **(3) Modularity comparison.** The weighted achieves higher modularity than the unweighted. The weighted is 0.58, and the unweighted is 0.49. In summary, utilizing regional power grid control, regional coupling degree, and modularity as evaluation metrics, the results indicate that constructing the power grid as a weighted reactive network can help improve the performance of power grid partitioning.

4.4.2. Enhanced Density Peak Model

The new local density and density following distance are designed for the enhanced density peak model in this paper. To demonstrate the superiority of the enhanced density peak model, three comparers are designed and conducted a comparison. The first comparer (EDPVP) is the EDPVP with the enhanced density peak model. The second comparer (EDPVP-other ρ) defines the degree of the nodes as the local density while keeping other aspects the same as in EDPVP. The third comparer (EDPVP-other δ) defines the number of hops between the nodes as the density following distance while maintaining the remaining aspects the same as in EDPVP. The evaluation of partition quality is based on regional power grid control, regional coupling degree, and modularity. The comparison results are shown in Figure 17 and Table 9.

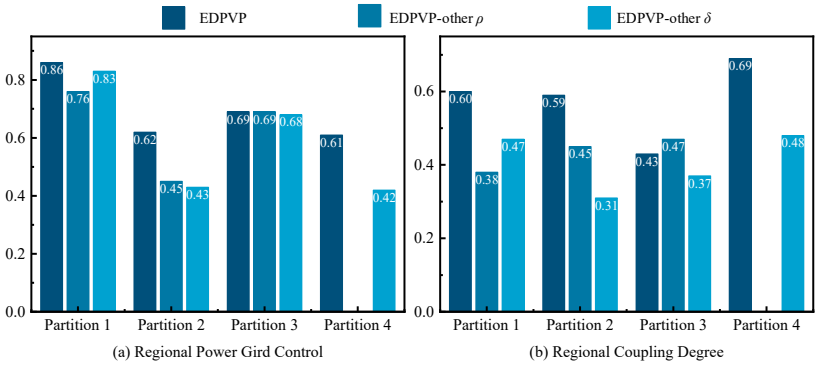


Figure 17. Comparison of the EDPVP with different ρ and δ.

Table 9. Modularity comparison of partitioning methods.

Partitioning Method	EDPVP	EDPVP-Other ρ	EDPVP-Other δ
Modularity	0.58	0.53	0.57

From Figure 17 and Table 9, a comparison of the EDPVP method with two strategies reveals the following findings: **(1) Regional power grid control comparison.** EDPVP outperforms EDPVP-other ρ and EDPVP-other δ in terms of regional power grid control in most partitions, except for Partition 3, where the values 0.69, 0.69, and 0.68 are relatively similar among the three methods. **(2) Regional coupling degree comparison.** EDPVP demonstrates higher regional coupling degrees in Partitions 1, 2, and 4 compared to EDPVP-other ρ and EDPVP-other δ. In Partition 3, the regional coupling degree of EDPVP is slightly lower than that of EDPVP-other ρ by 0.04. **(3) Modularity comparison.** EDPVP achieves higher modularity than both EDPVP-other ρ and EDPVP-other δ. In summary, utilizing regional power grid control, regional coupling degree, and modularity as evaluation metrics, the results indicate that the enhanced density peak model helps improve the performance of power grid partitioning.

5. Conclusions

This paper proposed the enhanced density peak-based power grid reactive voltage partitioning method (EDPVP), which can achieve accurate and robust reactive voltage partitioning. The method is as follows:

(1) The power grid is constructed as a weighted reactive network to take into account both the physical and electrical characteristics of different power-consuming entities in the power grid.

(2) The novel local density and density following distance are designed to make the density peak model adaptable for weighted reactive networks.

(3) An optimized cluster centers selection strategy and an updated remaining node assignment strategy are incorporated to make the reactive voltage partitioning robust and accurate.

The simulation experimental results on IEEE 39-bus system and IEEE 118-bus system confirmed that the proposed EDPVP method can improve the quality of the partitions and ensure enough reactive power reserve in each partition compared with other methods that do not consider the electrical characteristics thoroughly.

However, the effectiveness of EDPVP might vary depending on the characteristics of the power grid system under consideration, since we only analyzed the feasibility and advantages of the proposed method for the standard system and theoretically inferred its significance for solving engineering problems. In other words, its suitability might not be uniform across all types of power grid networks, and its performance could be influenced by the system's complexity and size. Additionally, the actual power grid is subject to dynamic changes in various factors, and further research is needed to determine the appropriate partitions in this situation.

Author Contributions: Conceptualization, X.D., C.L. and L.C.; writing—original draft, C.L.; formal analysis, C.L. and H.L.; supervision, C.L. and L.C.; validation, X.D., Y.G. and H.Z.; writing—reviewing and editing, X.D., H.L. and H.Z.; investigation, X.D., H.L. and Y.G.; visualization, L.C., Y.G. and H.Z.; resources, L.C.; methodology, Y.G., H.Z; data curation, H.Z. All authors have read and agreed to the published version of the manuscript.

Funding: This research is funded by the National Natural Science Foundation of China (No. 62103143); the Young Backbone Teacher of Hunan Province (No. 2022101); and the Scientific Research Fund of Hunan Provincial Education Department (No. 22B0471).

Data Availability Statement: Not applicable.

Conflicts of Interest: The authors declare no conflict of interest.

References

1. Xu, M.; Zhao, L.; Long, R.; Zhang, J.; Liu, Y.; Hu, H.; Tan, T.; Meng, Y.; Ma, W. Stability Analysis Method of AC/DC UHV Power System Based on Risk Assessment. In Proceedings of the 2016 5th International Conference on Civil, Architectural and Hydraulic Engineering (ICCAHE 2016), Zhuhai, China, 30–31 July 2016.
2. Gul, S.; Ul Haq, A.; Jalal, M.; Anjum, A.; Khalil, I.U. A unified approach for analysis of faults in different configurations of PV arrays and its impact on power grid. *Energies* **2019**, *13*, 156. [CrossRef]
3. Xiao, C.; Sun, L.; Ding, M. Multiple Spatiotemporal Characteristics-Based Zonal Voltage Control for High Penetrated PVs in Active Distribution Networks. *Energies* **2020**, *13*, 249. [CrossRef]
4. Chen, L.; Chen, F.; Liu, Z.; Lv, M.; He, T.; Zhang, S. Parallel gravitational clustering based on grid partitioning for large-scale data. *Appl. Intell.* **2022**, *53*, 2506–2526. [CrossRef]
5. Pan, G.; Wang, X.; Peng, X.; Wu, X. Study of power grid partition identification method based on community structure detection. *Power Syst. Prot. Control* **2013**, *41*, 116–121.
6. Zhao, J.; Liu, F.; Yong, D. Network Partitioning for Reactive Power/Voltage Control Based on a Mapping Division Algorithm. *Autom. Electr. Power Syst.* **2010**, *34*, 36–39.
7. Li, J.; Shang, X.; Wang, R. Soft measurement method of coal quantity for double-inlet and double-outlet mill based on clustering algorithm. *Therm. Power Gener.* **2020**, *49*, 114–119.
8. Huang, L. Research on the Community Discovery in Complex Network. *Microcomput. Appl.* **2017**, *33*, 11–12.
9. Wei, C.; Wei, Y.; Lee, W.; Xia, Z. Optimal Pilot-Bus Selection and Network Partitioning Algorithm Considering Zonal Reactive Power Balance. *Power Syst. Technol.* **2017**, *41*, 164–170.
10. Li, X.; Fu, X.; Zhu, J. Research on partition method and selection of dominant nodes for distribution network with distributed generation. *Power Syst. Prot. Control* **2019**, *47*, 24–29.
11. Zheng, J.; Zhong, J. A Complex Network Theory Fast Partition Algorithm of Reactive Voltage Based on Node Type and Coupling of Partitions. *Power Syst. Technol.* **2020**, *44*, 223–230.
12. Wang, Z.; Tan, W.; Li, H.; Ge, J.; Wang, W. A Voltage Coordination Control Strategy Based on the Reactive Power-Active Network Loss Partitioned Aggregation Domain. *Int. J. Electr. Power Energy Syst.* **2023**, *144*, 108585. [CrossRef]
13. Guo, Q.L.; Sun, H.B.; Zhang, B.M.; Wu, W.C. Power Network Partitioning Based on Clustering Analysis in Mvar Control Space. *Autom. Electr. Power Syst.* **2005**, *29*, 36–40+54.
14. Chen, L.; Guo, Q.; Liu, Z.; Zhang, S.; Zhang, H. Enhanced synchronization-inspired clustering for high-dimensional data. *Complex Intell. Syst.* **2021**, *7*, 203–223. [CrossRef]
15. Bao, W.; Zhu, T.; Zhao, C. A Three-stage Network Partition Method for Secondary Voltage Control Based on Agglomerative Analysis. *Autom. Electr. Power Syst.* **2016**, *40*, 127–132.
16. Biserica, M.; Foggia, G.; Chanzy, E.; Passelergue, J.C. Network partition for coordinated control in active distribution networks. In Proceedings of the 2013 IEEE Grenoble Conference, Grenoble, France, 16–20 June 2013; IEEE: Piscataway, NJ, USA, 2013; pp. 1–5.
17. Hasanvand, S.; Nayeripour, M.; Arefifar, S.A.; Fallahzadeh-Abarghouei, H. Spectral clustering for designing robust and reliable multi-MG smart distribution systems. *IET Gener. Transm. Distrib.* **2018**, *12*, 1359–1365. [CrossRef]
18. Znidi, F.; Davarikia, H.; Arani, M.; Barati, M. Coherency detection and network partitioning based on hierarchical DBSCAN. In Proceedings of the 2020 IEEE Texas Power and Energy Conference (TPEC), College Station, TX, USA, 6–7 February 2020; IEEE: Piscataway, NJ, USA, 2020; pp. 1–5.
19. Ankerst, M.; Breunig, M.M.; Kriegel, H.P.; Sander, J. OPTICS: Ordering points to identify the clustering structure. *ACM Sigmod Rec.* **1999**, *28*, 49–60. [CrossRef]
20. Rodriguez, A.; Laio, A. Clustering by fast search and find of density peaks. *Science* **2014**, *344*, 1492–1496. [CrossRef]
21. Wei, X.; Peng, M.; Huang, H.; Zhou, Y. An overview on density peaks clustering. *Neurocomputing* **2023**, *554*, 126633. [CrossRef]
22. Hou, J.; Zhang, A.; Qi, N. Density peak clustering based on relative density relationship. *Pattern Recognit.* **2020**, *108*, 107554. [CrossRef]
23. Chen, L.; Zheng, H.; Li, Y.; Liu, Z.; Zhao, L.; Tang, H. Enhanced density peak-based community detection algorithm. *J. Intell. Inf. Syst.* **2022**, *59*, 263–284. [CrossRef]
24. Chen, Y.; Hu, X.; Fan, W.; Shen, L.; Zhang, Z.; Liu, X.; Du, J.; Li, H.; Chen, Y.; Li, H. Fast density peak clustering for large scale data based on kNN. *Knowl.-Based Syst.* **2020**, *187*, 104824. [CrossRef]
25. Sun, L.; Ye, T.; Sun, J.; Duan, X.; Luo, Y. Density-Peak-Based Overlapping Community Detection Algorithm. *IEEE Trans. Comput. Soc. Syst.* **2021**, *9*, 1211–1223. [CrossRef]
26. Li, T.; Liang, X.; Jiang, F.; Feng, Z.; Zhang, K.; Cai, Z.; Gong, X.; Bai, X.; Li, M. Adaptive Dynamic Grid Partitioning for Reactive-Power/Voltage Control Based on Secondary Voltage Control. In *IOP Conference Series: Earth and Environmental Science*; IOP Publishing: Bristol, UK, 2019; Volume 300, p. 042109.
27. Cai, S.; Xie, Y.; Wu, Q.; Zhang, M.; Jin, X.; Xiang, Z. Active and reactive power coordinated two-stage MG scheduling for resilient distribution systems under uncertainties. *IEEE Trans. Smart Grid* **2022**, *13*, 2986–2998. [CrossRef]
28. Zhong, J.; Jiao, X.; Wang, Z. Reactive voltage partition method based on voltage critical steady state. *Power Syst. Technol.* **2019**, *43*, 3761–3768.
29. Ji, Y.; Xie, H.; Shi, S.; He, P.; Jin, N.; Wang, H. Voltage and Reactive Power Combinational Evaluation of Regional Power Grid Based on EWM-AHP-BP Neural Network. *J. Syst. Simul.* **2023**, *35*, 843.

30. Yoo, Y.; Jung, S.; Song, S.; Suh, J.; Lee, J.; Jang, G. Development of practical allocation method for reactive power reference for wind farms through inner-voltage restriction. *IET Gener. Transm. Distrib.* **2022**, *16*, 3069–3079. [CrossRef]
31. Tambunan, H.B.; Barus, D.H.; Hartono, J.; Alam, A.S.; Nugraha, D.A.; Usman, H.H.H. Electrical peak load clustering analysis using K-means algorithm and silhouette coefficient. In Proceedings of the 2020 International Conference on Technology and Policy in Energy and Electric Power (ICT-PEP), Bandung, Indonesia, 23–24 September 2020; IEEE: Piscataway, NJ, USA, 2020; pp. 258–262.
32. Newman, M.E.J.; Girvan, M. Finding and evaluating community structure in networks. *Phys. Rev. E* **2004**, *69*, 026113. [CrossRef]
33. Yang, B.; Yan, W.; Mo, J. Pilot-bus Selection and Network Partitioning Method Considering Randomness and Correlation of Source-Load Power. *Autom. Electr. Power Syst.* **2021**, *45*, 61–67.
34. Ge, H.; Guo, Q.; Sun, H.; Wang, B.; Zhang, B. Multivariate statistical analysis-based power-grid-partitioning method. *IET Gener. Transm. Distrib.* **2016**, *10*, 1023–1031. [CrossRef]
35. Xu, G.; Wang, Z. Fast Voltage Control Partitioning Based on Normal Matrix Spectral Bisection Method. *Power Syst. Technol.* **2014**, *38*, 199–204.
36. Li, W.; Tian, A.; Ma, J.; Mou, X.; Liang, X. Network partitioning approach for reactive power/voltage control using analytical nodes coupling expressions. *IET Gener. Transm. Distrib.* **2020**, *14*, 1337–1343. [CrossRef]

Disclaimer/Publisher's Note: The statements, opinions and data contained in all publications are solely those of the individual author(s) and contributor(s) and not of MDPI and/or the editor(s). MDPI and/or the editor(s) disclaim responsibility for any injury to people or property resulting from any ideas, methods, instructions or products referred to in the content.